AMERICAN SOCIETY FOR MICROBIOLOGY | Journal of Virology®

VACCINES AND ANTIVIRAL AGENTS

Intramuscular Immunization of Mice with the Live-Attenuated Herpes Simplex Virus 1 Vaccine Strain VC2 Expressing Equine Herpesvirus 1 (EHV-1) Glycoprotein D Generates Anti-EHV-1 Immune Responses in Mice

Shiliang A. Liu,[a] Brent A. Stanfield,[a] Vladimir N. Chouljenko,[a] Shan Naidu,[a] Ingeborg Langohr,[a] Fabio Del Piero,[a] Jacqueline Ferracone,[b] Alma A. Roy,[a] Konstantin G. Kousoulas[a]

Department of Pathobiological Sciences, School of Veterinary Medicine, Louisiana State University, Baton Rouge, Louisiana, USA[a]; Department of Clinical Studies and Pathology, University of Pennsylvania School of Veterinary Medicine, Philadelphia, Pennsylvania, USA[b]

ABSTRACT Vaccination remains the best option to combat equine herpesvirus 1 (EHV-1) infection, and several different strategies of vaccination have been investigated and developed over the past few decades. Herein, we report that the live-attenuated herpes simplex virus 1 (HSV-1) VC2 vaccine strain, which has been shown to be unable to enter into neurons and establish latency in mice, can be utilized as a vector for the heterologous expression of EHV-1 glycoprotein D (gD) and that the intramuscular immunization of mice results in strong antiviral humoral and cellular immune responses. The VC2–EHV-1–gD recombinant virus was constructed by inserting an EHV-1 gD expression cassette under the control of the cytomegalovirus immediate early promoter into the VC2 vector in place of the HSV-1 thymidine kinase (UL23) gene. The vaccines were introduced into mice through intramuscular injection. Vaccination with both the VC2–EHV-1–gD vaccine and the commercially available vaccine Vetera EHV^{XP} 1/4 (Vetera; Boehringer Ingelheim Vetmedica) resulted in the production of neutralizing antibodies, the levels of which were significantly higher in comparison to those in VC2- and mock-vaccinated animals ($P < 0.01$ or $P < 0.001$). Analysis of EHV-1-reactive IgG subtypes demonstrated that vaccination with the VC2–EHV-1–gD vaccine stimulated robust IgG1 and IgG2a antibodies after three vaccinations ($P < 0.001$). Interestingly, Vetera-vaccinated mice produced significantly higher levels of IgM than mice in the other groups before and after challenge ($P < 0.01$ or $P < 0.05$). Vaccination with VC2–EHV-1–gD stimulated strong cellular immune responses, characterized by the upregulation of both interferon- and tumor necrosis factor-positive CD4$^+$ T cells and CD8$^+$ T cells. Overall, the data suggest that the HSV-1 VC2 vaccine strain may be used as a viral vector for the vaccination of horses as well as, potentially, for the vaccination of other economically important animals.

IMPORTANCE A novel virus-vectored VC2–EHV-1–gD vaccine was constructed using the live-attenuated HSV-1 VC2 vaccine strain. This vaccine stimulated strong humoral and cellular immune responses in mice, suggesting that it could protect horses against EHV-1 infection.

KEYWORDS EHV-1, HSV-1, equine herpesvirus, live vector vaccines, glycoprotein D, immune response, mouse model

Received 18 December 2016 **Accepted** 14 March 2017

Accepted manuscript posted online 12 April 2017

Citation Liu SA, Stanfield BA, Chouljenko VN, Naidu S, Langohr I, Del Piero F, Ferracone J, Roy AA, Kousoulas KG. 2017. Intramuscular immunization of mice with the live-attenuated herpes simplex virus 1 vaccine strain VC2 expressing equine herpesvirus 1 (EHV-1) glycoprotein D generates anti-EHV-1 immune responses in mice. J Virol 91:e02445-16. https://doi.org/10.1128/JVI.02445-16.

Editor Richard M. Longnecker, Northwestern University

Address correspondence to Konstantin G. Kousoulas, vtgusk@lsu.edu.

Equine herpesvirus 1 (EHV-1) belongs to the *Alphaherpesvirinae* subfamily and is an important ubiquitous enzootic equine pathogen causing epidemic abortion, perinatal mortality, respiratory disease, and, occasionally, neurological disease in horses, resulting in significant economic losses to the horse industry. EHV-1 infection elicits a local immune response at the primary site of replication, as well as systemic humoral and cellular immune responses. EHV-1 infection of naive animals induces protective immunity against reinfection lasting 4 to 8 months after the initial acute infection (1). EHV-1 glycoproteins facilitate multiple aspects of the viral life cycle, including mediation of the fusion of the viral envelope with cellular membranes, intracellular virion morphogenesis, egress, cell-to-cell spread, and virus-induced cell fusion. Thus, these proteins are major antigenic determinants for both humoral and cellular immune responses and have been utilized as subunit vaccines (2–4). Specifically, immunization with EHV-1 glycoprotein D (gD) has been shown to generate protective immune responses in mice and horses (3, 5–11). EHV-1 and herpes simplex virus 1 (HSV-1) glycoproteins D are required for entry into cells and cell-to-cell fusion, a function which is conserved in most but not all alphaherpesviruses (12).

Despite regular and widespread vaccination, outbreaks of EHV-1 continue to occur. Current commercial vaccines that contain inactivated virus confer only partial clinical and virological protection against EHV-1 respiratory infections because they do not stimulate cellular immune responses, specifically, cytotoxic T cells that can control cell-associated viremia and virus dissemination from the respiratory tract (13). Virus-vectored vaccines express antigens within the infected cell that can be presented via major histocompatibility complex (MHC) class I (MHC-I; endogenous) and class II (MHC-II; exogenous) antigen-processing routes, stimulating both humoral and cell-mediated immune responses (14). Herein, we report the construction and testing of an effective HSV-1-vectored vaccine designed to prevent EHV-1 infections. The HSV-1 VC2 strain contains gK with the deletion of amino acids 31 to 68 and the deletion of the amino-terminal 19 amino acids of UL20, which render the virus unable to enter into the distal axons of ganglionic neurons, while the virus replicates efficiently in epithelial and fibroblast cells and generates robust and protective immune responses in mice (15) and guinea pigs (B. A. Stanfield and K. G. Kousoulas, unpublished data).

The mouse model of EHV-1 infection has been used to investigate the vaccine potentials of various EHV-1 immunogens, the effects of antiviral agents on EHV-1 infection, and the pathogenicities of EHV-1 strain variants and deletion or insertional mutants (16–18). The lung histopathology in EHV-1-infected mice is similar to that in infected horses and is characterized by an acute necrotizing alveolitis and bronchiolitis and eosinophilic intranuclear inclusion bodies in bronchiolar epithelial cells (19, 20). Although the mouse model of EHV-1 infection is not ideal, its extensive use has contributed toward the development of vaccine strategies. Herein, we show that the live-attenuated HSV-1 VC2 vaccine strain expressing EHV-1 gD can efficiently infect equine cells and generates strong and protective anti-EHV-1 immune responses in mice that may also protect horses against EHV-1 infection.

RESULTS

Construction and characterization of the VC2–EHV-1–gD vaccine. The EHV-1 gD gene under the control of the human cytomegalovirus (CMV) immediate early promoter was inserted in place of the thymidine kinase (UL23) gene (Fig. 1a). The gene insertion was verified by PCR-assisted sequencing of the insertion site, as well as by complete genomic sequencing of parental and mutant viral genomes (not shown) to ensure the absence of any spurious mutations. The virus was able to express the EHV-1 gD efficiently in both Vero and NBL-6 cells, as determined by the detection of both anti-gD-specific antibody and anti-FLAG antibody in Western immunoblots of infected cell extracts (Fig. 1b). VC2–EHV-1–gD replicated efficiently in both Vero and equine NBL-6 cells, approaching similar titers at 48 h postinfection (hpi) at both low and high multiplicities of infection (MOIs; 0.1 and 5, respectively) (Fig. 2). However, VC2–EHV-

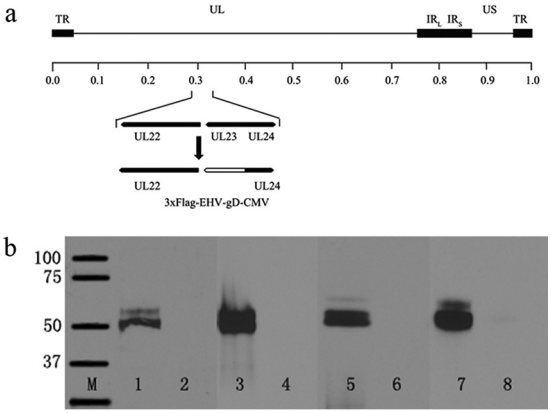

FIG 1 (a) Schematic of the VC2–EHV-1–gD genome. The schematic shows the insertion of the EHV-1 gD gene in place of the UL23 (thymidine kinase) gene. The 3× FLAG gene segment was inserted in frame to be expressed at the carboxyl terminus of gD. The locations of other relevant genes are shown. UL24, nuclear protein; TR, terminal repeat; UL, unique long region; IR_L, left inverted repeat; IR_R, right inverted repeat; US, unique short region. (b) Western immunoblots of gD expression. EHV-1 gD expression was detected by anti-FLAG antibodies or anti-EHV-1 gD 19-mer polyclonal antibodies (kindly provided by Dennis O'Callaghan, Louisiana State University Health Sciences Center, Shreveport, LA). Lanes 1 and 2, cellular extracts from VC2–EHV-1–gD- or VC2-infected NBL-6 cells detected by anti-FLAG antibody; lanes 3 and 4, cellular extracts from VC2–EHV-1–gD- or VC2-infected Vero cells detected by anti-FLAG antibody; lanes 5 and 6, cellular extracts from VC2–EHV-1–gD- or VC2-infected NBL-6 cells detected by a rabbit antibody generated against a 19-amino-acid peptide of EHV-1 gD; lanes 7 and 8, cellular extracts from VC2–EHV-1–gD- and VC2-infected Vero cells detected by anti-EHV-1 gD (19-mer); lane M, molecular mass markers (the numbers on the left are molecular masses [in kilodaltons]).

1–gD replicated significantly more slowly than the parental VC2 virus, reflected in their relative plaque sizes produced at 48 hpi (Fig. 3).

Monitoring of clinical disease symptoms. It has previously been reported that the parental VC2 vaccine strain did not produce any significant clinical disease after intramuscular administration in mice (15). Similarly, there were no adverse clinical signs noted after intramuscular injection of either VC2 or VC2–EHV-1–gD in mice throughout the vaccination period (8 weeks). In addition, during the vaccination period there were no significant weight differences among the groups (data not shown). The mice in all groups started to exhibit weight loss after challenge with wild-type EHV-1, although no clinical signs, such as fur ruffling and heavy breathing, were observed during the 6-week interval postchallenge. The unvaccinated group regained weight more slowly than the other three groups (Fig. 4).

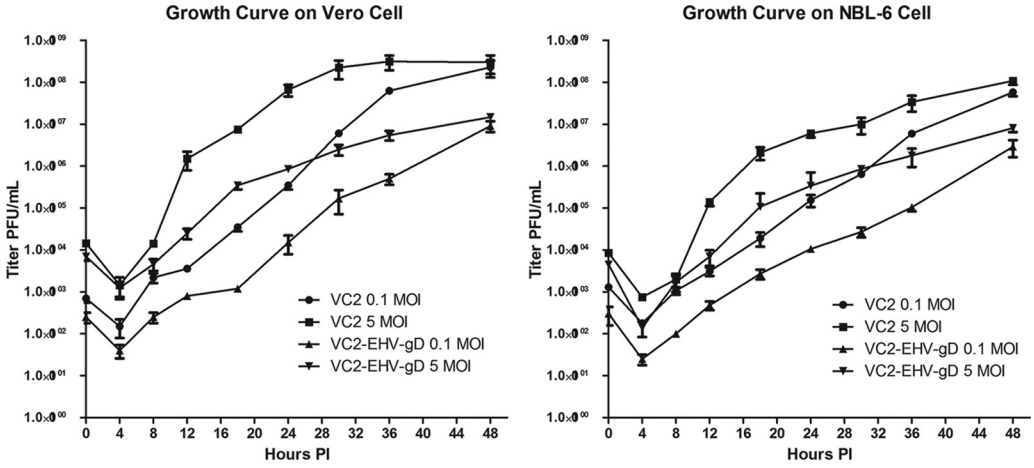

FIG 2 Replication kinetics of VC2 versus VC2–EHV-1–gD. Replication kinetics were produced for VC2 and VC2–EHV-1–gD at both a high MOI (MOI, 5) and a low MOI (MOI, 0.1) on Vero and NBL-6 cells.

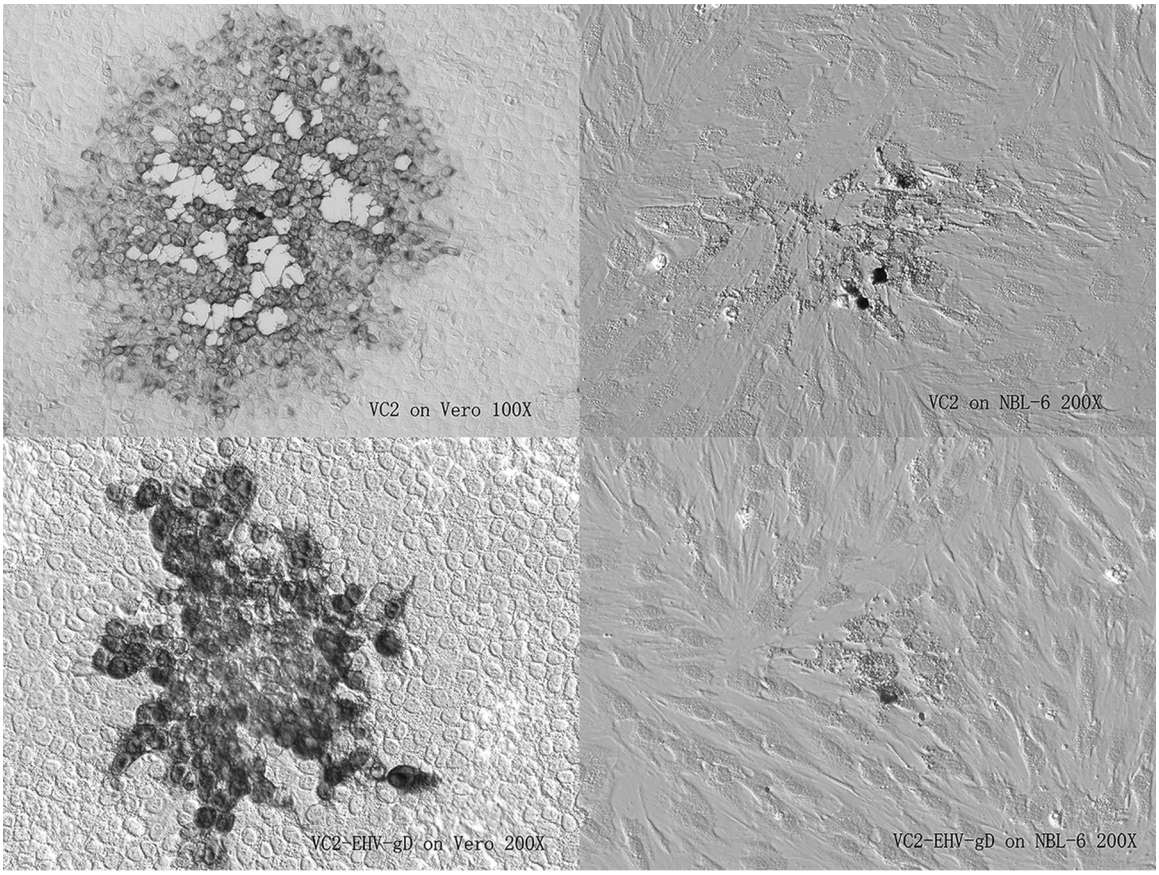

FIG 3 Plaque morphology of VC2 versus VC2-EHV-gD on Vero and NBL-6 cells at 72 h postinfection. Both viruses grew on Vero and NBL-6 cells, and VC2-EHV-gD produced smaller plaques than VC2.

Characterization of humoral immune responses. Antisera from all groups of mice were individually tested at a 1:20 dilution. A boost vaccination increased serum neutralization significantly. The animal groups vaccinated with the commercially available vaccine Vetera EHV^{XP} 1/4 (Vetera; Boehringer Ingelheim Vetmedica), VC2, and VC2–EHV-1–gD exhibited significantly higher virus-neutralizing (VN) activities than the

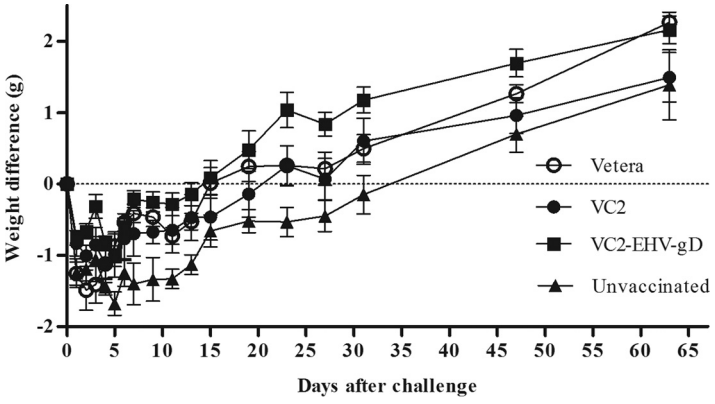

FIG 4 The effects of vaccination on the weights of mice in the Vetera-, VC2-, and VC2–EHV-1–gD-vaccinated groups and the unvaccinated groups were monitored daily after challenge with the EHV-1 clinical isolate. Statistical analyses of the differences between VC2–EHV-1–gD-vaccinated and unvaccinated mice were performed on day 7 ($P < 0.05$), day 9 ($P < 0.01$), day 11 ($P < 0.05$), day 23 ($P < 0.01$), day 27 ($P < 0.05$), and day 31 ($P < 0.05$). *P* values were determined by one-way analysis of variance followed by the Newman-Keuls multiple-comparison test.

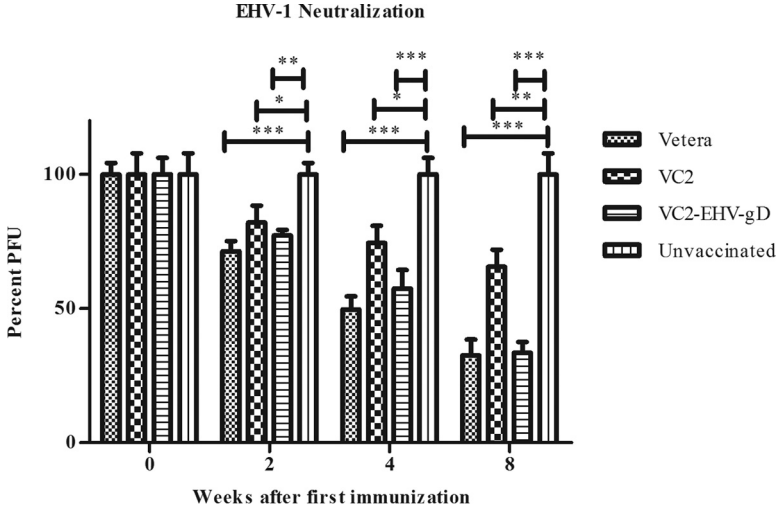

FIG 5 Virus-neutralizing activities. All serum samples were diluted 1:20 in growth medium and tested for the ability to neutralize approximately 100 PFU of EHV-1. Data were statistically analyzed by one-way analysis of variance followed by the Newman-Keuls multiple-comparison test. *, $P < 0.05$; **, $P < 0.01$; ***, $P < 0.001$.

unvaccinated group after the first immunization. VC2–EHV-1–gD vaccination increased the VN activity (33.6%) in mice after three consecutive vaccinations, and the VN activity was similar to that achieved with the commercial whole-virus vaccine (32.6%). Overall, the Vetera- and VC2–EHV-1–gD-vaccinated groups exhibited similar virus-neutralizing activities during the entire vaccination period, and these were significantly higher than those produced by the unvaccinated group ($P < 0.01$ or $P < 0.001$) and the VC2-vaccinated group at week 8 ($P < 0.01$) (Fig. 5).

Serum obtained from the VC2–EHV-1–gD-immunized group generated strong antigen-specific signals (Fig. 6a), which were significantly higher than those produced by the Vetera-vaccinated group ($P < 0.01$), the unvaccinated group ($P < 0.001$), and the VC2-vaccinated group ($P < 0.001$). Sera from all animals were also tested for their ability to detect EHV-1 antigens in infected Vero and NBL-6 cells. Sera from VC2-vaccinated animals demonstrated a higher reactivity in Vero and NBL-6 cells than sera from all other groups, in which reactivity was determined by indirect immunofluorescence to

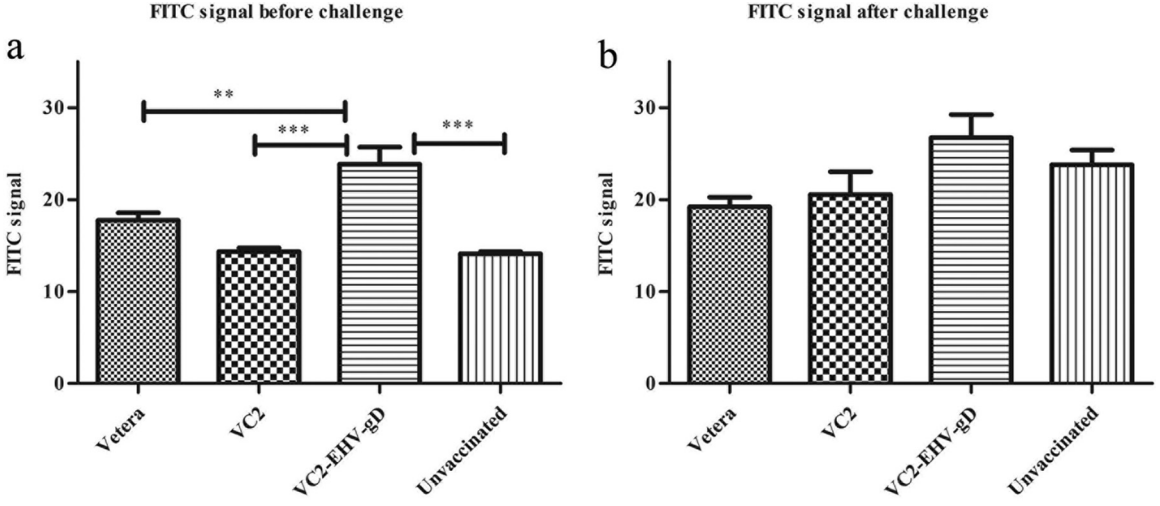

FIG 6 Anti-EHV-1 activities. Sera obtained from mice in the Vetera-, VC2-, and VC2–EHV-1–gD-vaccinated groups and the unvaccinated group before and after challenge were diluted 1:20 in growth medium and tested for their ability to react with EHV-1-infected RB13 cells. FACS data were analyzed by one-way analysis of variance followed by the Newman-Keuls multiple-comparison test. **, $P < 0.01$; ***, $P < 0.001$.

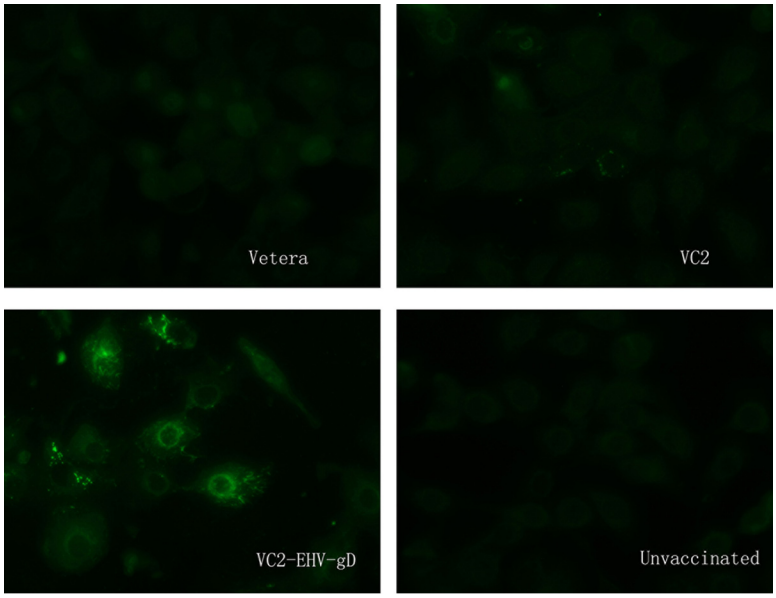

FIG 7 Anti-EHV-1 IFA assay. Sera obtained from mice in the Vetera-, VC2-, and VC2–EHV-1–gD-vaccinated groups and the unvaccinated group before challenge were diluted 1:20 and tested by the IFA assay.

assess the ability of serum from vaccinated and unvaccinated animals to detect EHV-1 antigens (Fig. 7). Overall, sera from the VC2–EHV-1–gD-immunized group produced the strongest EHV-1-specific IgG antibody signals when the signals from all groups were compared (Fig. 6b), in agreement with indirect fluorescent-antibody-facilitated detection of EHV-1 antigens in infected Vero and NBL-6 cells (Fig. 8).

The IgG1 levels produced in mice vaccinated with VC2–EHV-1–gD were significantly higher than those produced in the other groups of mice after three vaccinations and after challenge (Fig. 9a and b) ($P < 0.001$). The IgG2a levels in the VC2–EHV-1–gD-vaccinated group were also significantly higher than those in the other groups after three vaccinations (Fig. 9c and d) ($P < 0.001$), but there was no significant difference after EHV-1 challenge. Significantly more IgG2b was produced by the VC2–EHV-1–gD

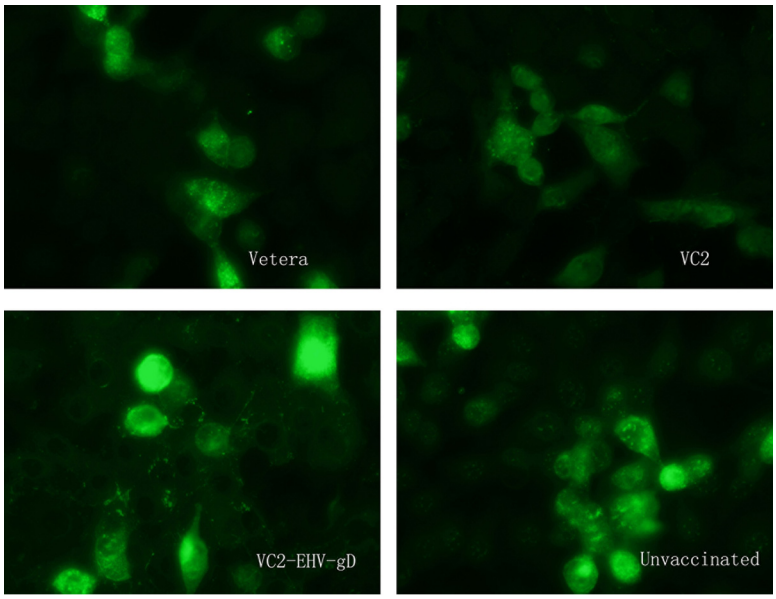

FIG 8 Anti-EHV-1 IFA assay. Sera obtained from mice in the Vetera-, VC2-, and VC2–EHV-1–gD-vaccinated groups and the unvaccinated group after challenge were diluted 1:20 and tested by the IFA assay.

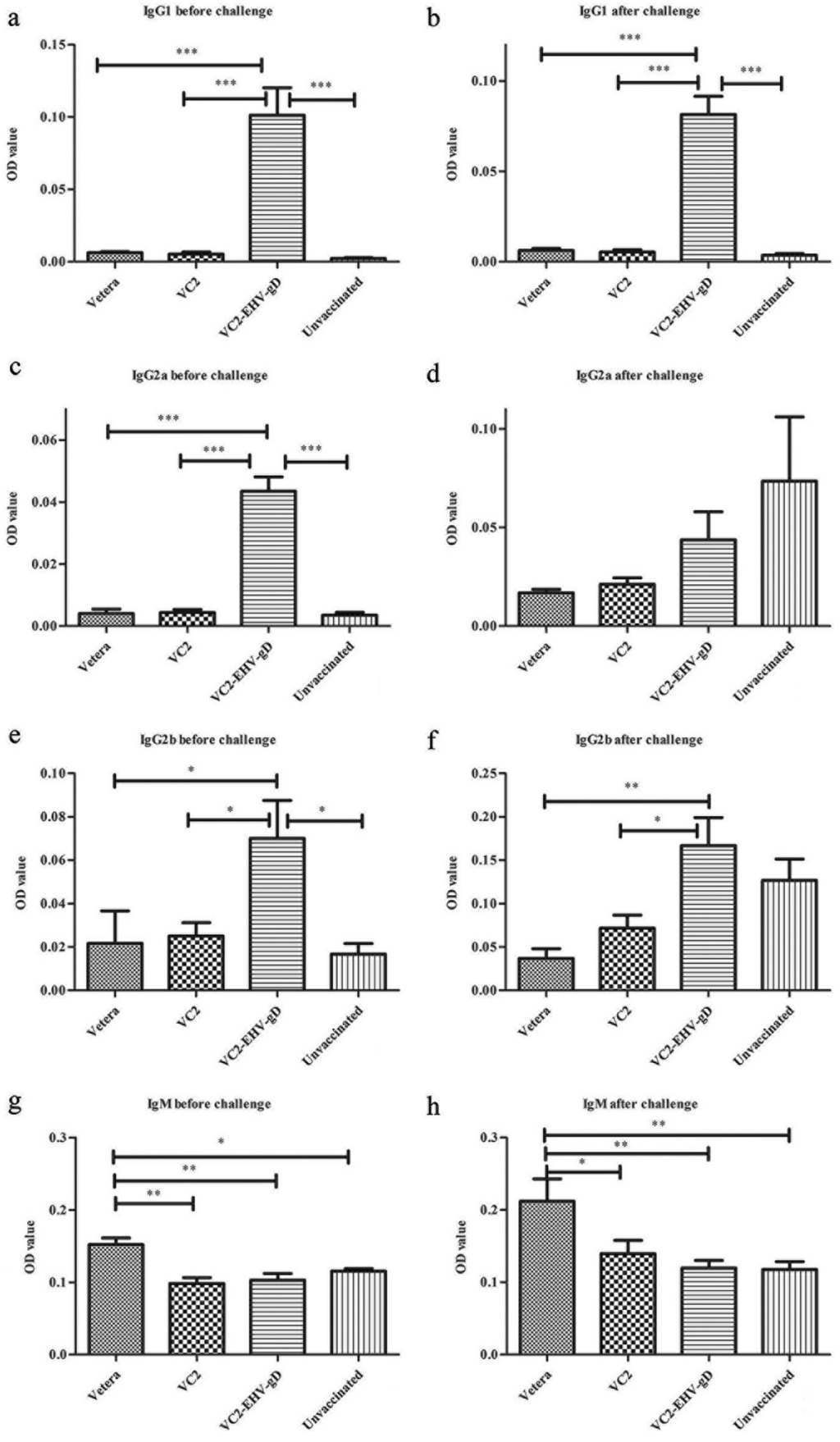
a
IgG1 before challenge
OD value
0.15
0.10
0.05
0.00
***
***
***
Vetera
VC2
VC2-EHV-gD
Unvaccinated
b
IgG1 after challenge
OD value
0.10
0.05
0.00
***
***
***
Vetera
VC2
VC2-EHV-gD
Unvaccinated
c
IgG2a before challenge
OD value
0.06
0.04
0.02
0.00
***
***
***
Vetera
VC2
VC2-EHV-gD
Unvaccinated
d
IgG2a after challenge
OD value
0.10
0.05
0.00
Vetera
VC2
VC2-EHV-gD
Unvaccinated
e
IgG2b before challenge
OD value
0.10
0.08
0.06
0.04
0.02
0.00
*
*
*
Vetera
VC2
VC2-EHV-gD
Unvaccinated
f
IgG2b after challenge
OD value
0.25
0.20
0.15
0.10
0.05
0.00
**
*
Vetera
VC2
VC2-EHV-gD
Unvaccinated
g
IgM before challenge
OD value
0.3
0.2
0.1
0.0
*
**
**
Vetera
VC2
VC2-EHV-gD
Unvaccinated
h
IgM after challenge
OD value
0.3
0.2
0.1
0.0
**
**
*
Vetera
VC2
VC2-EHV-gD
Unvaccinated

TABLE 1 Peptides predicted to be BALB/c mouse MHC-I and MHC-II binding epitopes

Peptide no.	MHC class	Allele	Length (no. of amino acids)	Position	Peptide sequence
1	I	H-2-Dd	12	338–349	KPPKTSKSNSTF
2	I	H-2-Ld	10	47–56	FPPPRYNYTI
3	II	H2-IEd	15	365–379	GVILYVCLRRKKELK

group than by the other groups ($P < 0.05$) after three vaccinations (Fig. 9e and f) ($P < 0.01$ or $P < 0.05$). Interestingly, Vetera-vaccinated animals produced significantly higher IgM levels than the other groups before and after challenge (Fig. 9g and h) ($P < 0.01$ or $P < 0.05$). No IgG3 or IgA was detected at a 1:100 dilution of serum from all treatment groups.

Cellular immune responses. A surface and intercellular labeling assay was utilized to detect the gamma interferon (IFN-γ) and tumor necrosis factor (TNF) synthesized by $CD4^+$ and $CD8^+$ T cells in the presence of specific peptides (Table 1) predicted to be MHC-I or MHC-II binding epitopes. All three peptides stimulated more IFN-γ-producing $CD4^+$ cells in the VC2- and VC2–EHV-1–gD-vaccinated groups than the Vetera-vaccinated and control groups after EHV-1 challenge. In the VC2–EHV-1–gD-vaccinated group, more IFN-γ-producing $CD8^+$ T cells were stimulated by peptide 1 or 3 after three vaccinations. Also, peptide 3 stimulated more IFN-γ-producing $CD8^+$ T cells in the Vetera-vaccinated group (Fig. 10). Moreover, all three peptides stimulated more IFN-γ-producing $CD8^+$ cells in the VC2–EHV-1–gD-vaccinated group after EHV-1 challenge. The peptides stimulated a cellular immune response after three vaccinations and postchallenge. There were more TNF-producing $CD8^+$ T cells in the VC2–EHV-1–gD-vaccinated group than in the other groups after stimulation of peripheral blood mononuclear cells (PBMCs) by all peptides (peptides 1, 2, and 3) at 1 week postchallenge (Fig. 11).

Immunohistochemistry of mouse lung tissues. Immunohistochemical analysis of the lung sections revealed a significant absence of EHV-1 antigen in the bronchiolar epithelial cells of the Vetera- and VC2–EHV-1–gD-vaccinated groups at 4 days after EHV-1 challenge (Fig. 12A and B). However, the lung tissues of the unvaccinated and VC2-vaccinated groups showed a prolonged presence of the EHV-1 antigen during the time period postchallenge. Interestingly, histopathological analysis revealed that, unlike the Vetera-vaccinated group, the pulmonary bronchioles and vasculature in the VC2–EHV-1–gD-vaccinated group were surrounded by reduced levels of inflammation at 4 days postchallenge in comparison to those in the VC2-vaccinated and unvaccinated groups (Fig. 12A and B).

DISCUSSION

In the study described here, we explored for the first time the use of the human herpes simplex virus 1 (HSV-1) VC2 vaccine strain as a potential live virus vaccine to combat EHV-1 infections. The VC2 virus was engineered to express the EHV-1 gD glycoprotein and was shown to elicit protective humoral and cellular immune responses in mice. The work suggests that the human HSV-1 VC2 vaccine strain may be utilized as a vector for the production of heterologous vaccines expressing immunogens that can protect horses and other animals against economically important pathogens.

The VC2-vaccinated group generated anti-EHV-1 neutralizing activity against EHV-1 infection, suggesting the presence of common immunogenic determinants between

FIG 9 *In vitro* analysis of the humoral immune response of the experimental groups. A colorimetric enzyme-linked immunosorbent assay was used to analyze a 1:100 dilution of serum from the Vetera-, VC2-, and VC2–EHV-1–gD-vaccinated mice and unvaccinated mice for EHV-1-reactive polyclonal IgG1, IgG2a, IgG2b, and IgM produced 8 weeks after the first vaccination (before challenge) and 1 week after challenge. Statistical comparisons were conducted using one-way analysis of variance followed by the Newman-Keuls multiple-comparison test. *, $P < 0.05$; **, $P < 0.01$; ***, $P < 0.001$. OD, optical density.

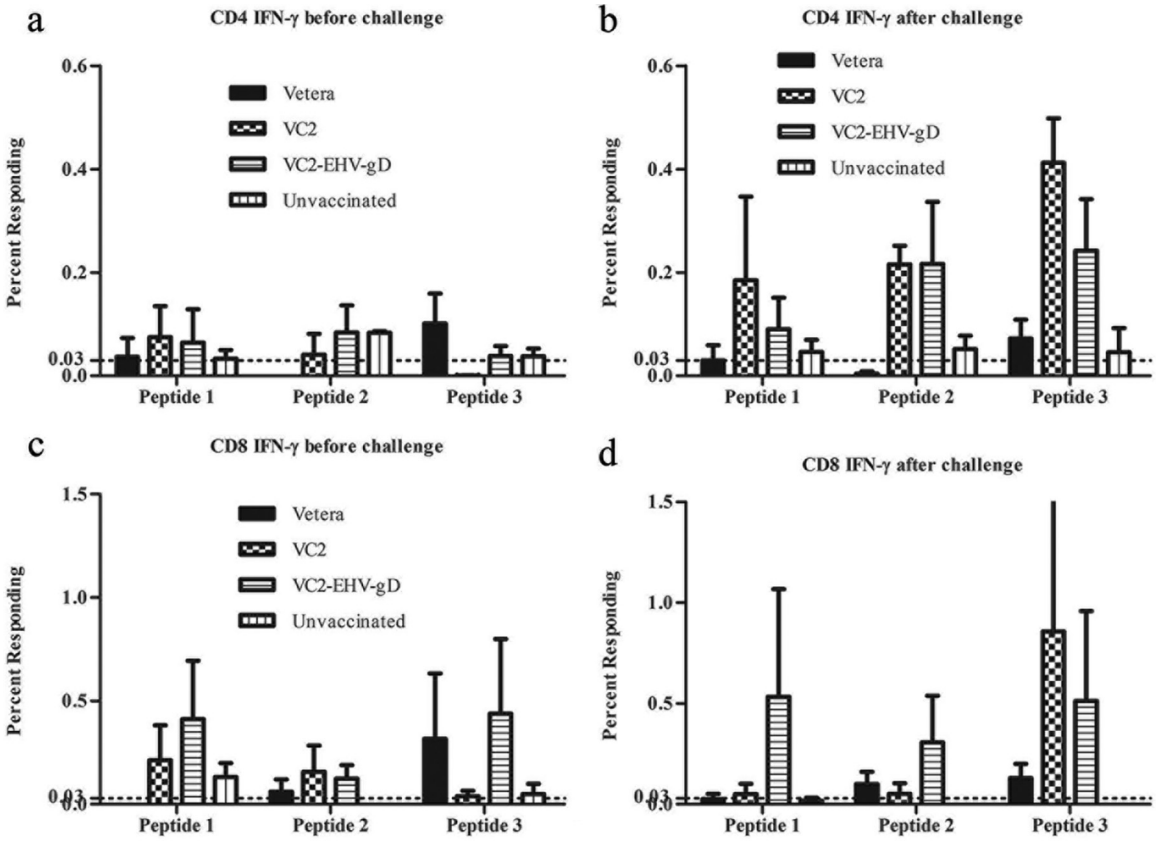

FIG 10 *In vitro* analysis of the cellular immune responses of the experimental groups. $CD4^+$ and $CD8^+$ T cells among splenocytes from the Vetera-, VC2-, and VC2–EHV-1–gD-vaccinated groups and the unvaccinated group were obtained after three vaccinations, stimulated with EHV-1 gD peptides, and analyzed by flow cytometry.

HSV-1 and EHV-1. HSV-1 and EHV-1 share a number of conserved genes and an overall genomic arrangement characteristic of the alphaherpesvirus subfamily. However, individual homologous viral proteins differ substantially in their primary sequences. Specifically, the HSV-1 and EHV-1 gDs exhibit 19.2% identity and 31.5% similarity. However, alignment of HSV-1 gD sequences indicates the conservation of certain continuous amino acid segments that could provide shared immunogenic responses. In addition, on the basis of the overall structure conservation of EHV-1 and HSV-1 gDs (21, 22), certain conformational epitopes may be conserved and may contribute to the observed cross-neutralizing activity of VC2. Also, it is likely that a number of other viral proteins may contribute immunogenic determinants that are common to strains and that produce cross-neutralizing activity. VC2–EHV-1–gD stimulated strong virus-neutralizing (VN) activity in comparison to that seen in both unvaccinated and VC2-vaccinated animals, and this VN activity was similar to that generated by the commercial EHV-1 killed virus vaccine. It has been reported that intranasal or intramuscular immunization with EHV-1 gD produces antigen-specific IgG responses (3, 4, 8, 10, 11, 22–25). In addition, the presence of VN antibody prior to EHV-1 infection was shown to be associated with a reduction in the amount and duration of nasopharyngeal virus shedding (26, 27). Flow cytometry tests revealed that VC2–EHV-1–gD stimulated significantly higher levels of specific anti-EHV-1 antibody than the commercial vaccine, suggesting that this response plays a major role in conferring protection against EHV-1 infection (Fig. 6) ($P < 0.001$). IgM antibodies are highly cross-reactive. They are typically produced early after an infection and are later replaced by higher-affinity IgG antibodies through isotype switching (28). Mice in the Vetera-vaccinated group produced anti-EHV-1 IgM at significantly higher levels than the other groups before and after challenge (Fig. 9) ($P < 0.05$ or $P < 0.01$), which may have contributed to the observed

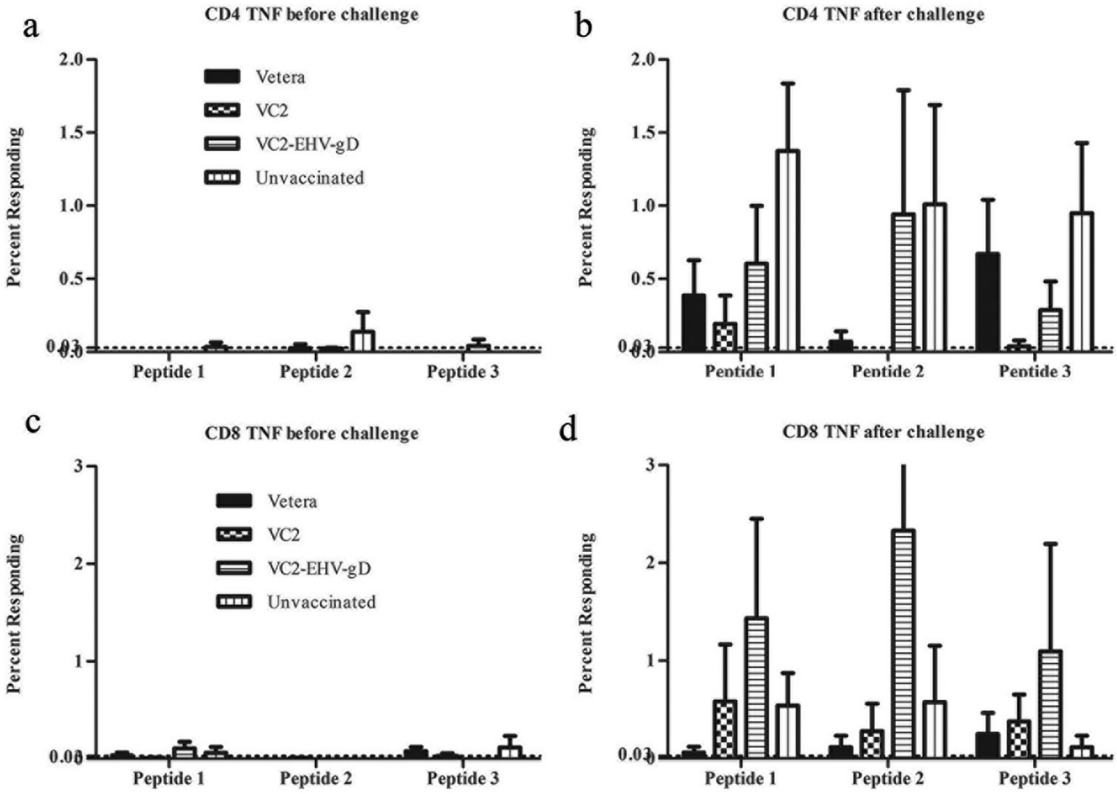

FIG 11 *In vitro* analysis of the cellular immune response of the experimental groups. $CD4^+$ and $CD8^+$ T cells among splenocytes from EHV-1-challenged mice from the Vetera-, VC2-, and VC2–EHV-1–gD-vaccinated groups and the unvaccinated group were stimulated with EHV-1 gD peptides (Table 1) and analyzed by flow cytometry.

virus-neutralizing activities (Fig. 5). However, the Vetera vaccine produced significantly lower anti-EHV-1 IgG levels than the VC2–EHV-1–gD vaccine (Fig. 6) ($P < 0.01$).

The IgG2a and IgG1 isotypes are markers for Th1 and Th2 responses, respectively (29–32). The IgG subclass induced after immunization or challenge is an indirect measure of the contribution of Th2-type cytokines relative to that of Th1-type cytokines. The production of IgG1-type antibodies is primarily induced by Th2-type cytokines, whereas the production of IgG2a-type antibodies reflects the involvement of Th1-type cytokines (33). These IgG subtypes were investigated in mice before and after EHV-1 challenge. The VC2–EHV-1–gD-vaccinated mice generated high IgG1 and IgG2a responses before challenge. However, IgG2a levels were enhanced after challenge, indicating a natural IgG2a response to EHV-1 infection. In comparison, mice in the other groups developed lower levels of IgG1 and IgG2a (Fig. 9). These results indicate that the VC2–EHV-1–gD vaccination generated a strong Th1 response priming the animals prior to challenge. Cytotoxic T lymphocytes (CTLs) are thought to be primarily responsible for eliminating EHV-1-infected cells (34–37). The VC2–EHV-1–gD vaccine increased the numbers of IFN-γ-producing $CD8^+$ cells after stimulation by peptide 3, indicating elicitation of anti-EHV-1 gD $CD8^+$ T cell responses (Fig. 10). IFN-γ is commonly produced by effector $CD8^+$ T lymphocytes, and upon recognition of the specific antigen, CTL activity can be measured (38, 39). Several studies conducted in mice have demonstrated an important role for IFN-γ in immune protection from herpesvirus infections (40, 41). Also, IFN-γ is critical for innate and adaptive immunity against viral infections in general and is an important activator of macrophages and an inducer of MHC molecule expression, while virus-specific $CD8^+$ T cells are thought to produce long-lived protection (42). After *in vitro* stimulation with EHV-1 gD peptides, equine PBMCs induced IFN-γ production by a significantly higher percentage of samples after EHV-1 infection than preinfection. This response was associated with an increase in virus-specific CTL activity, a critical immune

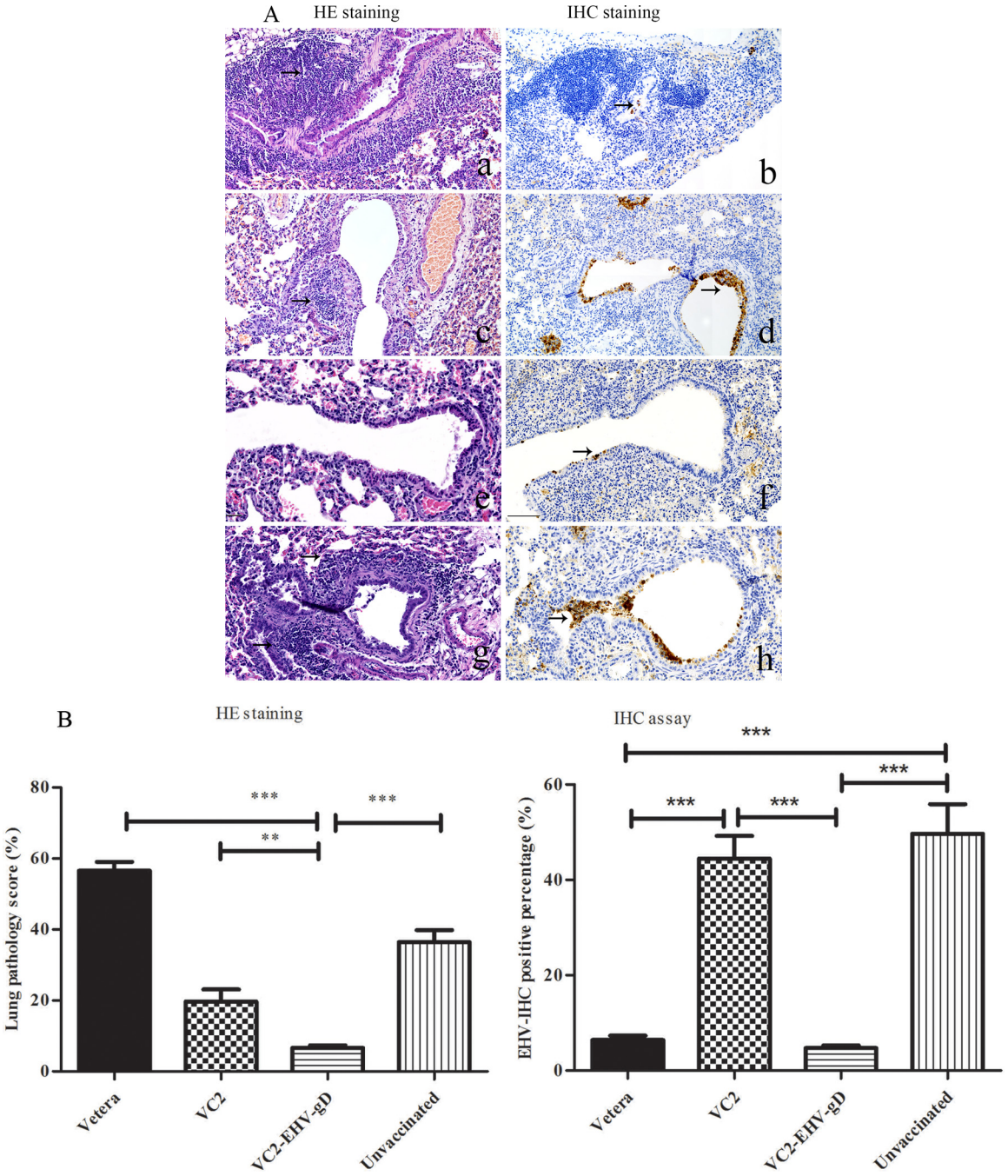

FIG 12 Histopathology of lung tissues. (A) Lung tissue showed intense inflammatory reactions (arrows) in the peribronchiolar and perivascular areas in the lung parenchyma at day 4 postchallenge. (Left) H&E-stained samples from mice vaccinated with Vetera (a), VC2 (c), or VC2–EHV-1–gD (e) and unvaccinated mice (g); (right) immunohistochemistry (IHC) staining of samples from mice vaccinated with Vetera (b), VC2 (d), or VC2–EHV-1–gD (f) and unvaccinated mice (h). Immunohistochemistry analysis shows that EHV-1 antigens were present in the infected bronchiolar cells lining the bronchioles (h, arrows). However, lung tissue from gD-vaccinated mice appeared histologically normal, with no appreciable amounts of viral antigens being detected (f, arrows). Photomicrographs were captured under a ×200 magnification. (B) Histopathology quantification. The degree of pulmonary inflammation in images of H&E-stained sections was quantified as the pathology score (percentage), as described in Materials and Methods (n = 3 mice/group). Immunohistochemistry staining was quantified as the percentage of EHV-1-positive bronchiolar epithelial cells in the lungs, as described in Materials and Methods (n = 3 mice/group).

effector for the control of EHV-1 infection and disease (43). Therefore, the observed $CD8^+$ T cell response generated by the VC2–EHV-1–gD vaccine must be a strong contributing factor limiting EHV-1 infection in mice. It remains to be tested whether similar immune responses can be generated in horses.

TABLE 2 Oligonucleotide primers used in this study

Primer	Template	Sequence[a]
P1	EHV-1 gD	AAGCTT**GCGGCCGCG**ATGTCTACCTTCAAGCTTATG
P2	EHV-1 gD	AAGCTT**GGATCC**CGGAAGCTGGGTATATTTAAC
P3	pEPkan-S	CTTGGT**GAATTC**AACTTCCCACAAGGAGAGCATATGACATGGTTGAAGTTCTGAGGATGACGACGATAAGTAGGG
P4	pEPkan-S	CTTGGT**GAATTC**CAACCAATTAACCAATTCTGATTAG
P5	CMV-14	GTGGCGTGAAACTCCCGCACCTCTTCGGCAAGCGCCTTGTAGAAGCGCGTCCATGTTGACATTGATTATTGAC
P6	CMV-14	TTATTGCCGTCATAGCGCGGGTTCCTTCCGGTATTGTCTCCTTCCGTGTTAAGGACAGGGAAGGGAGCAGTGG
P7	EHV-1 gD	GGCGTGTACGGTGGGAGGTCTATA
P8	EHV-1 gD	ATGCCAACGTGTGCAACGCCTATA
P9	EHV-1 gD	TTATGAAGCCCAGGCATTCGCAAG
P10	EHV-1 gD	AATTATGCCAACGTGTGCAACGC
P11	EHV-1 gD	CTGGTTCGTCTACGATGGTGGAA
P12	EHV-1 gD	AAGTCTGCACAGAACGGCTTGAC

[a]Boldface indicates restriction enzyme sites, and underlining indicates the sequences annealing to template.

Tumor necrosis factor (TNF) or tumor necrosis factor alpha (TNF-α) is an important cytokine that triggers local containment of infections. The VC2–EHV-1–gD vaccine group generated more TNF-producing $CD8^+$ T cells postchallenge than the other groups, which was in agreement with the findings described in a previous report that showed the concurrent upregulation of TNF transcripts postinfection in EHV-1 strain RacL11-infected mice (44). TNF stimulates endothelial cells to express proteins that trigger blood clotting in the local small vessels, occluding them and cutting off blood flow. This physiological effect may prevent the viruses from entering the bloodstream and spreading through the blood to organs all over the body, resulting in a reduction in the level of EHV-1 viremia. Further studies are needed to determine the specific role that TNF may play in the pathogenesis of EHV-1 infection.

Recently, the U.S. Food and Drug Administration (FDA) approved the Biologics License Application for talimogene laherparepvec (Imlygic), a genetically modified HSV-1 oncolytic viral therapy for the local treatment of unresectable cutaneous, subcutaneous, and nodal lesions in patients with recurrent melanoma after initial surgery. The HSV-1 VC2 strain has been shown to elicit robust humoral and cellular immune responses in mice, nonhuman primates, and guinea pigs and to confer protection against HSV-2 challenge in mice (15), nonhuman primates (45), and guinea pigs (B. A. Stanfield et al., unpublished data). Here, we describe the use of the VC2 virus for the production of a modified live-attenuated vaccine against EHV-1. It remains to be tested whether VC2 is safe for use by horses and other animals. The findings of those studies will pave the way for its use for the production of viral vector vaccines against major pathogens of economically important animal species.

MATERIALS AND METHODS

This work was approved by the Louisiana State University (LSU) Inter-Institutional Biological and Recombinant DNA Safety Committee (IBRDSC reference number 00615) and the Institutional Animal Care and Use Committee (IACUC reference number 15-019).

Virus and cells. A clinical EHV-1 strain was isolated from the placenta of a Thoroughbred horse in 2008 and provided by Alma Roy of the Louisiana Animal Disease Diagnostic Laboratory (LADDL). Vero (African green monkey kidney) and RK13 (rabbit kidney) cells were provided by LADDL and cultured using Dulbecco modified Eagle medium (DMEM) with 5% fetal bovine serum (FBS) and 1% antibiotic formulation (Primocin). NBL-6 (equine dermal) cells were purchased from ATCC and cultured/maintained as instructed by ATCC.

Construction of recombinant virus. The construction and characterization of HSV-1 VC2 have been described previously (15). The VC2 genome cloned into a bacterial artificial chromosome (BAC) plasmid was utilized for the construction of VC2–EHV-1–gD. The VC2 virus contains gK with the deletion of amino acids 31 to 68 as well as the deletion of the UL20 amino-terminal 19 amino acids (15). VC2 is unable to enter into neuronal endings, while it produces protective humoral and cellular immunity that fully protects vaccinated mice against HSV lethal disease (15). VC2–EHV-1–gD was constructed in *Escherichia coli* SW105 cells, using the two-step bacteriophage lambda Red-mediated recombination system, as described previously (15, 46). The EHV-1 gD sequence of 1,206 bp was amplified by PCR using primers P1 and P2 (Table 2). The PCR products were digested with the restriction enzymes NotI and BamHI and inserted into the vector CMV-14 with a 3× FLAG epitope inserted in frame at the carboxyl terminus of gD, resulting in recombinant plasmid CMV-gD. To construct CMV-gD-Kan^r, the kanamycin resistance (Kan^r) gene adjoining the I-SceI site was amplified by PCR from plasmid pEPkan-S using primers P3 and

TABLE 3 Vaccination design

Group[a]	Vaccine	Dose
1	Naive	No vaccination
2	Vetera EHV^{XP} 1/4[b]	0.1 ml for primary, secondary, and third boosts
3	VC2	10^5 PFU for primary, secondary, and third boosts
4	VC2–EHV-1–gD	10^5 PFU for primary, secondary, and third boosts

[a]Fifteen mice were included in each group.
[b]Vetera EHV^{XP} 1/4 (Boehringer Ingelheim Vetmedica) is an inactivated virus vaccine. It was diluted 1:1,000 in DMEM, and 0.1 ml was used as a single dose in mice.

P4 (Table 2), digested with the restriction enzyme EcoRI, and inserted into CMV-gD (digested with EcoRI). The CMV-gD-Kan^r gene was amplified by PCR using primers P5 and P6 (Table 2) and then cloned into VC2 to replace UL23 (thymidine kinase). The kanamycin resistance cassette was cleaved after expression of I-SceI from plasmid pBAD-I-SceI. The inserted EHV-1 gD was verified by capillary DNA sequencing by using primers P7 to P12 (Table 2).

Synthetic peptides. BALB/c mouse MHC-I and MHC-II binding peptides were predicted by the use of IEDB T cell epitope prediction tools (http://tools.immuneepitope.org/main/tcell/). The peptides were synthesized at the LSU Protein Core Lab (Table 1). These peptides (final concentration, 1 ng in each reaction tube) were used to stimulate splenocytes from different vaccinated or challenged mice *in vitro*.

Vaccination. Seven-week-old female BALB/c mice were used in this study (60 mice total; 4 groups of 15 mice each). Each mouse was identified with an ear tag. Naive animals did not get any vaccine, and the commercial vaccine Vetera EHV^{XP} 1/4 (Vetera; Boehringer Ingelheim Vetmedica), an inactivated virus vaccine, was used to immunize a control group of animals. Vaccines were administered intramuscularly (cranial thigh muscles) at 2-week intervals three times for all groups except the naive group (Table 3). Mice were observed and weighed daily over the course of the vaccination period. Blood/serum samples were collected from the facial vein every other week.

EHV-1 respiratory challenge in mice. Four groups of 11 mice each were challenged intranasally with 20 μl containing 5×10^7 PFU wild-type EHV-1 (10 μl per nostril) at 5 weeks following the final administration of the vaccine. Mice were weighed daily over the course of this study and were monitored daily for the development of clinical signs, such as ruffled fur, labored breathing, crouching or huddling behavior, sluggishness, and a loss of body weight. Previous research has demonstrated that body weight loss is an excellent indicator of EHV-1 infection in the mouse (47). Three mice from each group were sacrificed after 1 week for tissue collection and histopathological analysis.

Tissue collection and analysis. At 4 weeks after the 3rd vaccination and at 1 week postchallenge, three mice from each group were anesthetized by inhalation of 2 to 3% isoflurane. The total blood volume of each mouse was collected, and the mice were euthanized by cervical dislocation. The blood was allowed to clot at room temperature for at least 30 min. Serum was centrifuged, collected, and stored at −20°C until use. The spleens were excised from the euthanized animals, minced, and passed through a 10-mm-mesh-size nylon mesh cell strainer in RPMI 1640 medium with 10% heat-inactivated fetal bovine serum (HI-FBS). Cell suspensions were pelleted by centrifugation at $400 \times g$ for 7 min, and the cell concentration was adjusted to 10^7 cells/ml for fluorescence-activated cell sorting (FACS) analysis. After challenge, the lung tissues from all four groups were collected and fixed in 10% formalin for immunohistochemistry.

Serum neutralization. The collected serum was used to neutralize 50 μl of approximately 100 PFU of EHV-1. After the serum samples were heated to 56°C for 1 h to inactivate complement, samples were then diluted 1:10 in complete DMEM containing 10% heat-inactivated FBS. Fifty microliters of virus was added to each dilution of serum to a total volume of 100 μl. The addition of the virus made the final serum dilution 1:20. Serum-virus mixtures were placed on a rocker at room temperature for 1 h and titrated on NBL-6 cell monolayers.

FITC flow cytometry analysis with mouse serum. RK13 cells were infected with EHV-1 and were disassociated by using 1 mM EDTA in phosphate-buffered saline (PBS). Fixation/permeabilization solution was then added to the cells. Serum (1:20) from mice in the different groups was mixed with the cells after two washes, and the mixture was incubated for 30 min at 37°C. Goat anti-mouse antibody conjugated with fluorescein isothiocyanate (FITC) was added to the suspension, and the mixture was incubated for another 30 min at 37°C. The cells were washed twice by adding 3 ml buffer (1% HI-FBS in PBS). BD fixative solution was applied to the cells, and the cells were kept at 4°C until flow cytometry analysis.

IFA analysis of mouse serum. Serum samples (1:20) from the mice in the different groups were placed on equine herpesvirus 1 indirect fluorescent-antibody (IFA) slides (catalog no. SLD-IFA-ERV; Veterinary Medical Research & Development [VMRD]), and the slides were incubated for 30 min at 37°C. An anti-equine IgG-FITC conjugate (catalog no. 043-10; VMRD) was added to the slides, and the slides were incubated for another 30 min at 37°C after they were washed. The slides were observed under a Nikon fluorescence microscope.

Characterization of antibody subclass. To determine the antigen-specific antibody isotypes, 96-well plates were coated with 50 μl of EHV-1-infected cell lysate (20 μl/ml), and then serum from each of the four groups of animals was diluted 1:100 and tested in duplicate. To detect the mouse IgG1, IgG2a, IgG2b, IgG3, IgA, and IgM isotypes, anti-mouse IgG subclass-specific horseradish peroxidase-conjugated secondary antibodies (1/10,000 dilution; Abcam) were used.

Analysis of immune responses using polychromatic flow cytometry. The spleens were excised from euthanized animals, minced, and passed through a 10-mm-mesh-size nylon mesh cell strainer

(Fisher Scientific) in RPMI 1640 medium containing 10% HI-FBS and 1% Primocin. The cell suspensions were then pelleted by centrifugation at 400 × *g* for 7 min at 4°C. Five milliliters of ammonium chloride-potassium (ACK) lysing buffer was added to the cells. The cells were suspended and kept at room temperature for 7 min, and then the volumes were adjusted to a total of 25 ml with RPMI 1640 medium. The cell concentration was adjusted to 10^7 cells/ml after the cells were washed with RPMI 1640 medium. Three different peptides (1 ng), 3 μl Golgi-Plus, and 100 μl of the splenocyte suspension (10^7 cells/ml) were gently mixed. Then, the mixtures were incubated at 37°C and the splenocytes were stimulated for 6 h. The cells were then stained with monoclonal rat anti-mouse CD3 antibody conjugated to peridinin chlorophyll protein-Cy5.5 (BD Biosciences), monoclonal rat anti-mouse CD4 antibody conjugated to phycoerythrin (BD Biosciences), rat anti-mouse CD8a antibody conjugated to FITC (BD Biosciences), monoclonal rat anti-mouse IFN-γ antibody conjugated to allophycocyanin (BD Biosciences), and rat anti-mouse TNF antibody conjugated to BV510 (BD Biosciences). FACS was performed using an Accuri C6 personal flow cytometer. The data were analyzed using FlowJo software (v10.1r1; FlowJo Enterprise).

Immunohistochemistry assay. Lung tissue samples were fixed in 10% formalin, dehydrated through increasing ethanol gradients, and paraffin embedded, before 4-μm sections were obtained for hematoxylin and eosin (H&E) staining and immunohistochemical assays. The EHV-1 glycoprotein G1 was detected using a rabbit anti-EHV-1 monoclonal murine antibody (courtesy of George Allen [now deceased]), and the secondary antibody used was a goat anti-mouse IgG antibody (Abcam, USA). Finally, the slides were visualized using a light microscope (Nikon, Japan) and pictured using an Olympus DP72 camera. The slides were analyzed and scored for cellular inflammation under a light microscope by a pathologist who was blind to the treatment groups, as previously described (48). Briefly, inflammatory infiltrates were scored by enumerating the layers of inflammatory cells surrounding the vessels and bronchioles. Zero to three layers of inflammatory cells were considered normal. Moderate to abundant amounts of infiltrate (more than three layers of inflammatory cells surrounding 50% or more of the circumference of the vessel or bronchioles) were considered abnormal. The number of abnormal perivascular and peribronchial spaces divided by the total number of perivascular and peribronchial spaces was the percentage reported as the pathology score. A total of up to 20 perivascular and peribronchial spaces per lung were randomly selected and counted for each animal. Similarly, immunohistochemical staining was scored as the percentage of positively stained bronchiolar cells and adjacent vascular endothelial cells. A total of approximately 70 to 100 bronchiolar epithelial cells and peribronchiolar vascular endothelial cells were counted for each lung tissue section.

ACKNOWLEDGMENTS

We acknowledge the assistance provided by the staff of the Division of Biotechnology & Molecular Medicine and the Department of Biological Sciences, College of Basic Sciences, Louisiana State University. We acknowledge critical reviews of the manuscript by Paul Rider.

S.A.L. was supported by funds from the Louisiana Veterinary Diagnostic Laboratory. The work was supported by the Division of Biotechnology & Molecular Medicine and Cores of the Center for Experimental Infectious Disease Research (CEIDR), supported by the NIH, NIGMS, grant P30GM110670.

REFERENCES

1. Trapp S, von Einem J, Hofmann H, Kostler J, Wild J, Wagner R, Beer M, Osterrieder N. 2005. Potential of equine herpesvirus 1 as a vector for immunization. J Virol 79:5445–5454. https://doi.org/10.1128/JVI.79.9.5445-5454.2005.
2. Laval K, Favoreel HW, Poelaert KC, Van Cleemput J, Nauwynck HJ. 2015. Equine herpesvirus type 1 enhances viral replication in CD172a$^+$ monocytic cells upon adhesion to endothelial cells. J Virol 89:10912–10923. https://doi.org/10.1128/JVI.01589-15.
3. Fuentealba N, Sguazza G, Scrochi M, Bravi M, Zanuzzi C, Corva S, Gimeno E, Pecoraro M, Galosi C. 2014. Production of equine herpesvirus 1 recombinant glycoprotein D and development of an agar gel immunodiffusion test for serological diagnosis. J Virol Methods 202:15–18. https://doi.org/10.1016/j.jviromet.2014.02.025.
4. Fuentealba NA, Zanuzzi CN, Scrochi MR, Sguazza GH, Bravi ME, Cid de la Paz V, Corva SG, Portiansky EL, Gimeno EJ, Barbeito CG, Galosi CM. 2014. Protective effects of intranasal immunization with recombinant glycoprotein D in pregnant BALB/c mice challenged with different strains of equine herpesvirus 1. J Comp Pathol 151:384–393. https://doi.org/10.1016/j.jcpa.2014.06.003.
5. Packiarajah P, Walker C, Gilkerson J, Whalley JM, Love DN. 1998. Immune responses and protective efficacy of recombinant baculovirus-expressed glycoproteins of equine herpesvirus 1 (EHV-1) gB, gC and gD alone or in combinations in BALB/c mice. Vet Microbiol 61:261–278. https://doi.org/10.1016/S0378-1135(98)00189-8.
6. Zhang Y, Smith PM, Tarbet EB, Osterrieder N, Jennings SR, O'Callaghan DJ. 1998. Protective immunity against equine herpesvirus type-1 (EHV-1) infection in mice induced by recombinant EHV-1 gD. Virus Res 56:11–24. https://doi.org/10.1016/S0168-1702(98)00054-9.
7. Azab W, Osterrieder N. 2012. Glycoproteins D of equine herpesvirus type 1 (EHV-1) and EHV-4 determine cellular tropism independently of integrins. J Virol 86:2031–2044. https://doi.org/10.1128/JVI.06555-11.
8. Weerasinghe CU, Learmonth GS, Gilkerson JR, Foote CE, Wellington JE, Whalley JM. 2006. Equine herpesvirus 1 glycoprotein D expressed in E. coli provides partial protection against equine herpesvirus infection in mice and elicits virus-neutralizing antibodies in the horse. Vet Immunol Immunopathol 111:59–66. https://doi.org/10.1016/j.vetimm.2006.01.009.
9. Foote CE, Raidal SL, Pecenpetelovska G, Wellington JE, Whalley JM. 2006. Inoculation of mares and very young foals with EHV-1 glycoproteins D and B reduces virus shedding following respiratory challenge with EHV-1. Vet Immunol Immunopathol 111:97–108. https://doi.org/10.1016/j.vetimm.2006.01.012.
10. Foote CE, Love DN, Gilkerson JR, Rota J, Trevor-Jones P, Ruitenberg KM, Wellington JE, Whalley JM. 2005. Serum antibody responses to equine herpesvirus 1 glycoprotein D in horses, pregnant mares and young foals. Vet Immunol Immunopathol 105:47–57. https://doi.org/10.1016/j.vetimm.2004.12.012.
11. Ruitenberg KM, Gilkerson JR, Wellington JE, Love DN, Whalley JM. 2001. Equine herpesvirus 1 glycoprotein D expressed in Pichia pastoris is

hyperglycosylated and elicits a protective immune response in the mouse model of EHV-1 disease. Virus Res 79:125–135. https://doi.org/10.1016/S0168-1702(01)00337-9.
12. Csellner H, Walker C, Wellington JE, McLure LE, Love DN, Whalley JM. 2000. EHV-1 glycoprotein D (EHV-1 gD) is required for virus entry and cell-cell fusion, and an EHV-1 gD deletion mutant induces a protective immune response in mice. Arch Virol 145:2371–2385. https://doi.org/10.1007/s007050070027.
13. Kydd JH, Townsend HG, Hannant D. 2006. The equine immune response to equine herpesvirus-1: the virus and its vaccines. Vet Immunol Immunopathol 111:15–30. https://doi.org/10.1016/j.vetimm.2006.01.005.
14. Yeo WM, Osterrieder N, Stokol T. 2013. Equine herpesvirus type 1 infection induces procoagulant activity in equine monocytes. Vet Res 44:16. https://doi.org/10.1186/1297-9716-44-16.
15. Stanfield BA, Stahl J, Chouljenko VN, Subramanian R, Charles AS, Saied AA, Walker JD, Kousoulas KG. 2014. A single intramuscular vaccination of mice with the HSV-1 VC2 virus with mutations in the glycoprotein K and the membrane protein UL20 confers full protection against lethal intravaginal challenge with virulent HSV-1 and HSV-2 strains. PLoS One 9:e109890. https://doi.org/10.1371/journal.pone.0109890.
16. Walker C, Love DN, Whalley JM. 1999. Comparison of the pathogenesis of acute equine herpesvirus 1 (EHV-1) infection in the horse and the mouse model: a review. Vet Microbiol 68:3–13. https://doi.org/10.1016/S0378-1135(99)00056-5.
17. Frampton AR, Jr, Smith PM, Zhang Y, Grafton WD, Matsumura T, Osterrieder N, O'Callaghan DJ. 2004. Meningoencephalitis in mice infected with an equine herpesvirus 1 strain KyA recombinant expressing glycoprotein I and glycoprotein E. Virus Genes 29:9–17. https://doi.org/10.1023/B:VIRU.0000032785.19420.14.
18. Ma G, Eschbaumer M, Said A, Hoffmann B, Beer M, Osterrieder N. 2012. An equine herpesvirus type 1 (EHV-1) expressing VP2 and VP5 of serotype 8 bluetongue virus (BTV-8) induces protection in a murine infection model. PLoS One 7:e34425. https://doi.org/10.1371/journal.pone.0034425.
19. Bartels MJ, McNett DA, Timchalk C, Mendrala AL, Christenson WR, Sangha GK, Brzak KA, Shabrang SN. 1998. Comparative metabolism of ortho-phenylphenol in mouse, rat and man. Xenobiotica 28:579–594. https://doi.org/10.1080/004982598239335.
20. Bartels T, Steinbach F, Hahn G, Ludwig H, Borchers K. 1998. In situ study on the pathogenesis and immune reaction of equine herpesvirus type 1 (EHV-1) infections in mice. Immunology 93:329–334.
21. Wellington JE, Lawrence GL, Love DN, Whalley JM. 1996. Expression and characterization of equine herpesvirus 1 glycoprotein D in mammalian cell lines. Arch Virol 141:1785–1793. https://doi.org/10.1007/BF01718301.
22. Flowers CC, O'Callaghan DJ. 1992. Equine herpesvirus 1 glycoprotein D: mapping of the transcript and a neutralization epitope. J Virol 66:6451–6460.
23. Ruitenberg KM, Love DN, Gilkerson JR, Wellington JE, Whalley JM. 2000. Equine herpesvirus 1 (EHV-1) glycoprotein D DNA inoculation in horses with pre-existing EHV-1/EHV-4 antibody. Vet Microbiol 76:117–127. https://doi.org/10.1016/S0378-1135(00)00237-6.
24. Ruitenberg KM, Walker C, Wellington JE, Love DN, Whalley JM. 1999. DNA-mediated immunization with glycoprotein D of equine herpesvirus 1 (EHV-1) in a murine model of EHV-1 respiratory infection. Vaccine 17:237–244. https://doi.org/10.1016/S0264-410X(98)00192-3.
25. Love DN, Bell CW, Whalley JM. 1992. Characterization of the glycoprotein D gene products of equine herpesvirus 1 using a prokaryotic cell expression vector. Vet Microbiol 30:387–394. https://doi.org/10.1016/0378-1135(92)90024-N.
26. Kydd JH, Wattrang E, Hannant D. 2003. Pre-infection frequencies of equine herpesvirus-1 specific, cytotoxic T lymphocytes correlate with protection against abortion following experimental infection of pregnant mares. Vet Immunol Immunopathol 96:207–217. https://doi.org/10.1016/j.vetimm.2003.08.004.
27. Hannant D, Jessett DM, O'Neill T, Dolby CA, Cook RF, Mumford JA. 1993. Responses of ponies to equid herpesvirus-1 ISCOM vaccination and challenge with virus of the homologous strain. Res Vet Sci 54:299–305. https://doi.org/10.1016/0034-5288(93)90126-Z.
28. Bego MG, Bawiec D, Dandge D, Martino B, Dearing D, Wilson E, St Jeor S. 2008. Development of an ELISA to detect Sin Nombre virus-specific IgM from deer mice (Peromyscus maniculatus). J Virol Methods 151:204–210. https://doi.org/10.1016/j.jviromet.2008.05.008.
29. Song N, Lu F, Huang S, Ding G, Zhou Z, Liao Z. 2014. Effect of aqueous extracts of Scutellaria baicalensis Georgi and Radix paeoniae Alba on the serum IgG1 and IgG2a of the periodontitis mice. Zhonghua Kou Qiang Yi Xue Za Zhi 49:89–94. (In Chinese.)
30. Ebrahimpoor S, Pakzad SR, Ajdary S. 2013. IgG1 and IgG2a profile of serum antibodies to Leishmania major amastigote in BALB/c and C57BL/6 mice. Iran J Allergy Asthma Immunol 12:361–367.
31. Koyama K, Ito Y. 2001. Comparative studies on the levels of serum IgG1 and IgG2a in susceptible B10.BR mice infected with different strains of the intestinal nematode parasite Trichuris muris. Parasitol Res 87:570–572. https://doi.org/10.1007/s004360000351.
32. Berger A. 2000. Th1 and Th2 responses: what are they? BMJ 321:424. https://doi.org/10.1136/bmj.321.7258.424.
33. Yadav D, Khuller G. 2001. Evaluation of the T cells and costimulatory molecules in the protective efficacy of 30 kDa secretory protein against experimental tuberculosis. Immunol Cell Biol 79:207–212. https://doi.org/10.1046/j.1440-1711.2001.00998.x.
34. Soboll G, Whalley JM, Koen MT, Allen GP, Fraser DG, Macklin MD, Swain WF, Lunn DP. 2003. Identification of equine herpesvirus-1 antigens recognized by cytotoxic T lymphocytes. J Gen Virol 84:2625–2634. https://doi.org/10.1099/vir.0.19268-0.
35. Allen GP, Kydd JH, Slater JD, Smith KC. 2004. Equid herpesvirus 1 and equid herpesvirus 4 infections. Infect Dis Livestock 76:829–859.
36. Allen GP, Bolin DC, Bryant U, Carter CN, Giles RC, Harrison LR, Hong CB, Jackson CB, Poonacha K, Wharton R, Williams NM. 2008. Prevalence of latent, neuropathogenic equine herpesvirus-1 in the Thoroughbred broodmare population of central Kentucky. Equine Vet J 40:105–110. https://doi.org/10.2746/042516408X253127.
37. Allen G, Yeargan M, Costa LR, Cross R. 1995. Major histocompatibility complex class I-restricted cytotoxic T-lymphocyte responses in horses infected with equine herpesvirus 1. J Virol 69:606–612.
38. O'Flaherty BM, Matar CG, Wakeman BS, Garcia A, Wilke CA, Courtney CL, Moore BB, Speck SH. 2015. $CD8^+$ T cell response to gammaherpesvirus infection mediates inflammation and fibrosis in interferon gamma receptor-deficient mice. PLoS One 10:e0135719. https://doi.org/10.1371/journal.pone.0135719.
39. McCarthy MK, Procario MC, Twisselmann N, Wilkinson JE, Archambeau AJ, Michele DE, Day SM, Weinberg JB. 2015. Proinflammatory effects of interferon gamma in mouse adenovirus 1 myocarditis. J Virol 89:468–479. https://doi.org/10.1128/JVI.02077-14.
40. Mikloska Z, Cunningham AL. 2001. Alpha and gamma interferons inhibit herpes simplex virus type 1 infection and spread in epidermal cells after axonal transmission. J Virol 75:11821–11826. https://doi.org/10.1128/JVI.75.23.11821-11826.2001.
41. Cantin E, Tanamachi B, Openshaw H. 1999. Role for gamma interferon in control of herpes simplex virus type 1 reactivation. J Virol 73:3418–3423.
42. Shin H, Iwasaki A. 2012. A vaccine strategy that protects against genital herpes by establishing local memory T cells. Nature 491:463–467. https://doi.org/10.1038/nature11522.
43. Breathnach CC, Soboll G, Suresh M, Lunn DP. 2005. Equine herpesvirus-1 infection induces IFN-gamma production by equine T lymphocyte subsets. Vet Immunol Immunopathol 103:207–215. https://doi.org/10.1016/j.vetimm.2004.09.024.
44. Smith PM, Zhang Y, Grafton WD, Jennings SR, O'Callaghan DJ. 2000. Severe murine lung immunopathology elicited by the pathogenic equine herpesvirus 1 strain RacL11 correlates with early production of macrophage inflammatory proteins 1alpha, 1beta, and 2 and tumor necrosis factor alpha. J Virol 74:10034–10040. https://doi.org/10.1128/JVI.74.21.10034-10040.2000.
45. Stanfield BA, Pahar B, Chouljenko VN, Veazey R, Kousoulas KG. 2017. Vaccination of rhesus macaques with the live-attenuated HSV-1 vaccine VC2 stimulates the proliferation of mucosal T cells and germinal center responses resulting in sustained production of highly neutralizing antibodies. Vaccine 35:536–543. https://doi.org/10.1016/j.vaccine.2016.12.018.
46. Tischer BK, von Einem J, Kaufer B, Osterrieder N. 2006. Two-step Red-mediated recombination for versatile high-efficiency markerless DNA manipulation in Escherichia coli. Biotechniques 40:191–197. https://doi.org/10.2144/000112096.
47. van Woensel PA, Goovaerts D, Markx D, Visser N. 1995. A mouse model for testing the pathogenicity of equine herpes virus-1 strains. J Virol Methods 54:39–49. https://doi.org/10.1016/0166-0934(95)00024-O.
48. Haeberle HA, Kuziel WA, Dieterich HJ, Casola A, Gatalica Z, Garofalo RP. 2001. Inducible expression of inflammatory chemokines in respiratory syncytial virus-infected mice: role of MIP-1alpha in lung pathology. J Virol 75:878–890. https://doi.org/10.1128/JVI.75.2.878-890.2001.